Acoustic Environment in Large Enclosures With a Small Opening Exposed to Flow

Leonard Shaw*
Flight Dynamics Laboratory, Wright-Patterson Air Force Base, Ohio
and
Harold Bartel† and James McAvoy‡
Lockheed-Georgia Co., Marietta, Georgia

The acoustic environment in large enclosures with a small opening exposed to aerodynamic flow has been quantified. Theoretical/empirical techniques were developed for predicting the oscillatory frequencies, acoustic pressure level, spatial distribution of the acoustic pressures in the cavity, and the degree of alleviation achievable with suppressors. Experimental tests in a semifree jet facility were performed on scale models of large enclosures. The test Mach numbers ranged from 0.4 to 1.2. Levels as high as 184 dB were measured in the test enclosures. Acoustic resonant modes as high as 15 were observed. Numerous turbulence generating suppressors were evaluated. The results showed that size, location, and orientation had more influence on the effectiveness of the suppressors than the degree of turbulence generated. Suppressor optimization resulted in more than 30 dB of suppression for one configuration.

Introduction

IT is a well-known fact that aerodynamic flow past an opening in an enclosure will generate an acoustic environment in the enclosure. Everyone can associate with the classic case of "blowing over a pop bottle" or the increase in the noise inside an automobile when a window is opened at higher speeds. These examples are at low flow speeds relative to applications of flow-induced cavity pressure fluctuations in aircraft. The speed range of interest in aircraft goes from landing speeds up to and including supersonic speeds. At these speeds the fluctuating pressure level in an enclosure can be high enough to cause structural failures in whatever is stored in the enclosure or the structure of the enclosure itself. Thus it is desirable to be able to predict the fluctuating pressure levels that will occur in enclosures and have techniques to suppress the high levels.

Most of the past research has concentrated on cavities with a large opening exposed to freestream flow. Typically the opening would be one entire wall of the cavity. Some of the prediction and suppression methodologies developed for that class of flow-induced cavity oscillations cannot be applied to large enclosures with small openings. Some of the earliest investigations of cavity resonance were directed toward quantifying the noise radiated away from cavities, with analytical prediction techniques becoming available in the early 1960s. In 1962, Plumblee, Gibson, and Lassiter[1] developed a method to predict cavity response based on a strong mathematical treatment, with results supported by model tests. They hypothesized that acoustic modes within the cavity were driven by boundary-layer turbulence resulting in intense pressure fluctuations. Subsequent efforts to apply the method of Plumblee et al. proved their method to be more applicable to what later became defined as "deep" cavities. Notably, though, the method provides a way to calculate depthwise as well as lengthwise acoustic modes in a rectangular enclosure having one entire wall open to high-speed flow.

Presented as Paper 82-0121 at the AIAA 20th Aerospace Sciences Meeting, Orlando, Fla., Jan. 11-14, 1982; submitted Jan. 19, 1982; revision received May 17, 1982. This paper is declared a work of the U.S. Government and therefore is in the public domain.

*Aerospace Engineer, Acoustics and Sonic Fatigue Group. Member AIAA.
†Staff Engineer, Structures Technology Division.
‡Staff Engineer, Structures Technology Division. Member AIAA.

In 1964, J. E. Rossiter[2] conducted experiments that identified the source of excitation as vortices shedding from the upstream edge of the aperture. He formulated an analytical expression for the cavity oscillation frequency that has been widely used for "shallow" cavities. In 1970, Heller, Holmes, and Covert[3] modified and improved Rossiter's frequency formula to correct for the speed of sound in the cavities. In 1975, Smith and Shaw[4] formulated an empirical sound pressure level prediction scheme which was based on extensive flight test data. In 1976, Bliss and Hayden[5] presented expressions for the fluctuating pressure and total power radiated from cavities. Shaw and Smith[6] in 1977 presented measured levels from full scale flight tests which added credence to small scale test data validity. NASA-sponsored work has been done by Block and Tam[7,8] concerning, among other things, the extension of Rossiter's work to predict cavity oscillations below Mach 0.4 for cavities such as open landing gear wheel wells. Considerable work on cavity oscillations has also been contributed by the academic community, dealing with cavity oscillations in aerospace vehicles, wind tunnel walls, and ships.

In 1978, Rockwell and Naudascher[9] correlated the modes obtained by Rossiter in his original work (for $L/D=2$) with the longitudinal acoustic resonance in Rossiter's cavity. They assumed that all six walls were hard and neglected depth mode response. Improved correlation is obtained when the modified Rossiter formula is used in conjuction with a more precise accounting of the acoustic resonances.

Only a small percent of the numerous past investigators have studied suppression techniques. Heller and Bliss[10] presented several concepts which were shown to be effective suppressors. Shaw[11] presented flight data which displayed the effectiveness of leading-edge spoilers.

The current effort reviewed the prediction and suppression concepts developed over the years for enclosures with large openings for their applicability to large enclosures with small openings. Despite the broad range of data reviewed, very little information was found to be directly applicable to large enclosures. Thus the prediction methods developed in this paper relied mostly on theory and scale model test data.

Test Facility

The principal feature of the test facility was a semifree cold air rectangular jet nozzle with an integral flow-plane, capable

of continuous operation at velocities exceeding Mach 1.2. The overall arrangement is shown in Fig. 1.

A flow-plane which contained the aperture was adjacent to one wall of the nozzle and was mounted in a vertical plane. A flow fence made of heavy aluminum tooling plate was positioned on each side of the aperture to form, in conjunction with the flow-plane, a deep channel projecting downstream from the nozzle exit. This channel arrangment constrained the flow on three sides while allowing expansion and secondary air entrainment opposite the aperture. It produced the effect of a divergent nozzle at the aperture without having a wall opposite the aperture to reflect pressure fluctuations or cause acoustic resonance effects. The aperture (or opening) in the flow-plane was located slightly downstream of the nozzle exit (see Fig. 1). The velocity distribution across the aperture was considerably improved over that available from a freejet nozzle, as speed over the aperture deviated less than 1% from the velocity at the center of the aperture for all speeds below Mach 1.0. The width of the flowfield over the aperture was three times the aperture width. The depth of the flowfield over the aperture was 1.3 times the aperture length. The flow-plane thickness at the aperture was 0.080 in. The models were attached to the back side of the flow-plane, with their opening positioned over the flow-plane aperture. Thus the models were outside the flow to avoid physical interference with the airstream.

Test Models

The cavity models had either cylindrical or rectangular cross sections with relocatable end plugs and removable floors which provided variation in cavity length, neck length, and opening location either upstream or downstream. For all model configurations the small opening measured 1×6 in. One rectangular configuration had an opening the same width as the cavity which yielded data that could be compared to existing prediction methods. The rectangular model is shown in Fig. 2 and the cylindrical one in Fig. 3. The removable floor is also shown in Fig. 3. The models were constructed either from ¾-in. plywood, ½-in. plexiglass, or rolled aluminum sheet. In every case checks were made to verify that structural vibrations did not contribute to the oscillatory pressure response of the models.

Instrumentation

The instrumentation and the test procedures were tailored to define sound pressure spectra inside the enclosures over a Mach range of from 0.4 to 1.2 and a dynamic pressure range of from 200-2000 psf.

Microphones (¼ in.) were located inside the models to sense pressure fluctuations. In some instances, the microphones were permanently fixed in the models. For spatial surveys, the microphones were mounted in tubular probes that were repositioned in discrete increments. The microphone signals were amplified or attenuated as necessary for maximum signal-to-noise ratio, using B&K Model 2603 microphone amplifiers. The microphone data analysis was done on-line with Nicolet Scientific Corporation Model 446A Fast Fourier Transform computing analyzers and companion digital plotters.

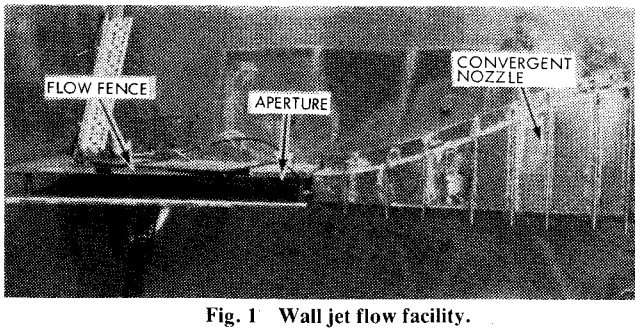

Fig. 1 Wall jet flow facility.

The cavity response and the properties of the flow were recorded at stabilized flow conditions. The frequency response spectra were continuously monitored on a scope display for on-line identification of critical velocities where response changes and response maxima occurred. Total head and static pressure sensors were mounted in the flowstream in the vicinity of the aperture.

Test Results

Typical spectra from a cylindrical cavity are shown in Fig. 4. Data are shown for Mach numbers from 0.43 to 1.15. The microphone was located at the downstream end of the cavity on the wall opposite of the openings. The analysis bandwidth, 12.5 Hz, was small enough to distinguish the very narrowband cavity oscillations. The figure reveals that specific oscillation modes prefer specific Mach numbers. As Mach number increases some modes are suppressed while other modes are amplified. It should be noted that the highest amplitudes are experienced near Mach 1. Similar data for a rectangular cavity are shown in Fig. 5.

It has been shown in several references[3,4,10] that the flow-induced acoustic resonant modes in an enclosure exhibit spatial mode shapes. A movable microphone was used to obtain data at various longitudinal locations. The results of one survey are presented in Fig. 6. The theoretical cosine curves shown in the figure descend to zero at the modes but the measured data descend only to the broadband noise floor, which averaged about 135 dB. The broadband noise also adds to the level of the oscillations to some extent on each side of the modes, which tends to flatten the mode shapes. In general the data verify the spatial distributions observed in other tests.

Derivation of Prediction

The solid lines in Fig. 7 show the cavity oscillation frequency vs Mach number obtained with the modified

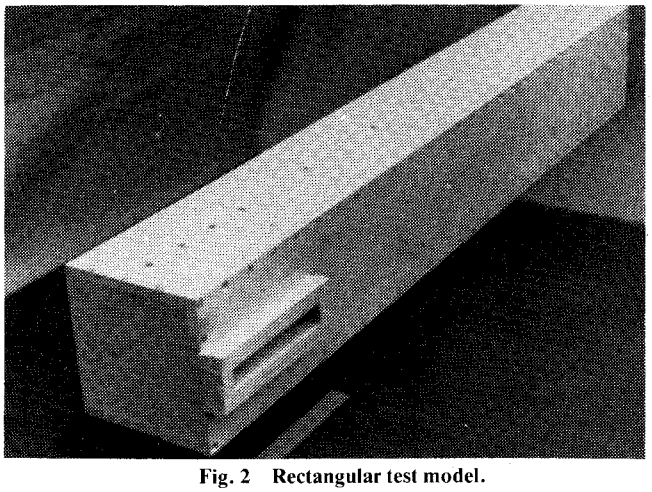

Fig. 2 Rectangular test model.

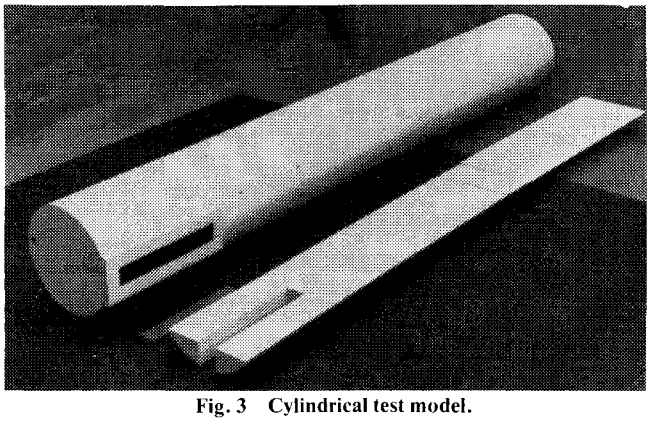

Fig. 3 Cylindrical test model.

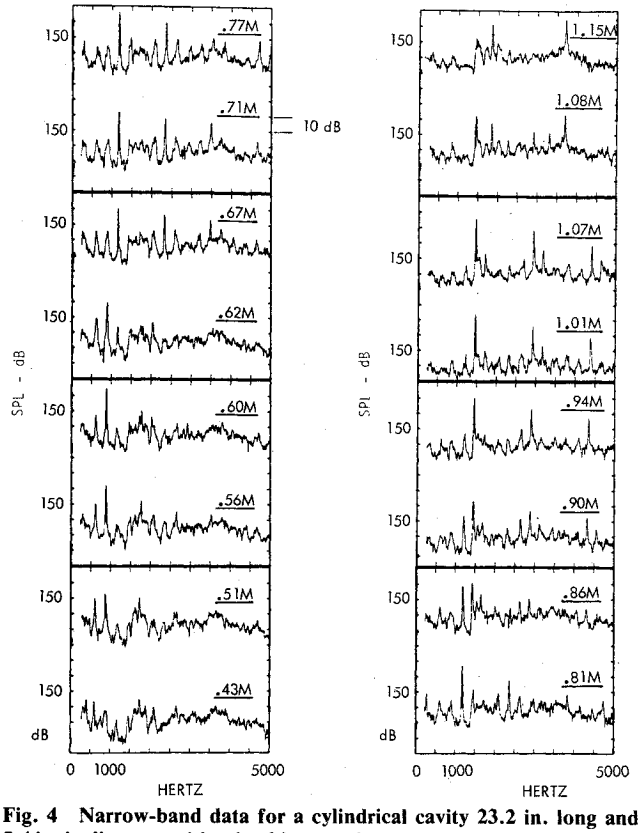

Fig. 4 Narrow-band data for a cylindrical cavity 23.2 in. long and 5.4 in. in diameter with a 1×6-in. opening.

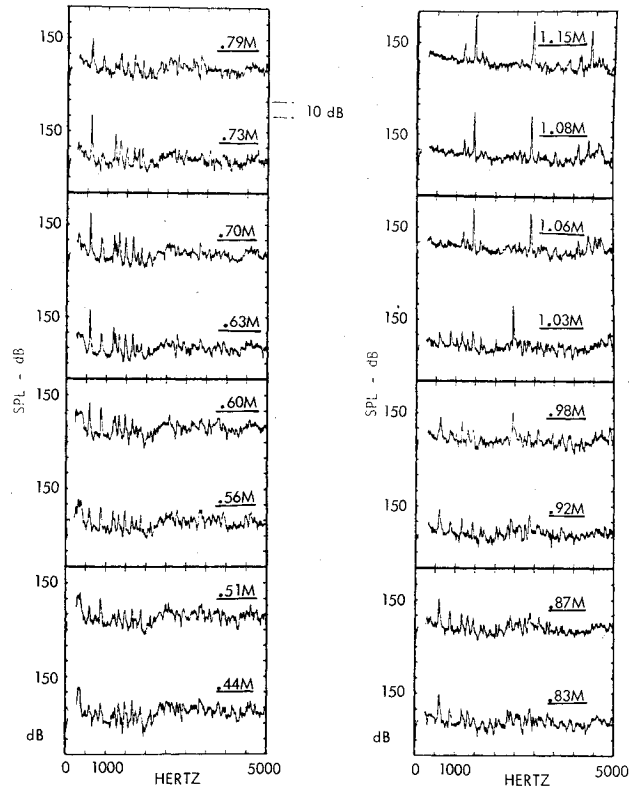

Fig. 5 Narrow-band data for a rectangular cavity 23.2 in. long, 5.75×5.75 in.^{2}, with a 1×6-in. opening.

Rossiter[3] equation for the first three modal orders ($N_R = 1$, 2, and 3). The modified Rossiter equation is

$$f = \frac{U_\infty}{L} \frac{N_R - \alpha_R}{M(1+0.2M^2)^{-1/2} + 1/K_v} \tag{1}$$

For moderate cavity length-to-depth ratios and flow velocities above about $0.5M$, the appropriate values for the constants α_R and K_V are 0.25 and 0.057, respectively; U_∞ is the freestream velocity; L is the aperture length; N_R is the modal integer (1, 2, 3, etc.); and M is the freestream Mach number. The cavity oscillation frequency given by the Spee[12,13] equation is also shown in Fig. 7 for the first three modal orders. The Spee equation is

$$\tan\frac{2\pi f N_s L}{U_c} = \frac{2\pi f N_s L}{U_c} \tag{2}$$

where U_c is shear layer particle velocity in this convection velocity, which Rossiter suggested to be 57% of freestream velocity. While the Spee relation gave fair agreement with the data in this comparison, it generally did not fit the data as well as the Rossiter equation.

The modified Rossiter equation was therefore preferred in subsequent data correlations. Figure 7 also shows that, while the cavity oscillation frequency may coincide roughly with any of the first three modal orders given by the Rossiter equation, there is no indication of which mode responds for a given cavity and flow condition. There is also considerable scatter in the data. Thus the frequency of oscillation is not predicted accurately with the modified Rossiter equation alone.

A detailed study of the data revealed that as velocity was increased to the point where cavity oscillation occurred, the frequency of oscillation often remained nearly constant, generally coinciding with one of the cavity acoustic resonances through a broad speed range.

An illustration of this is shown in Fig. 8 for a rectangular 18×5.75×5.75-in. cavity model having a 1×6-in. aperture

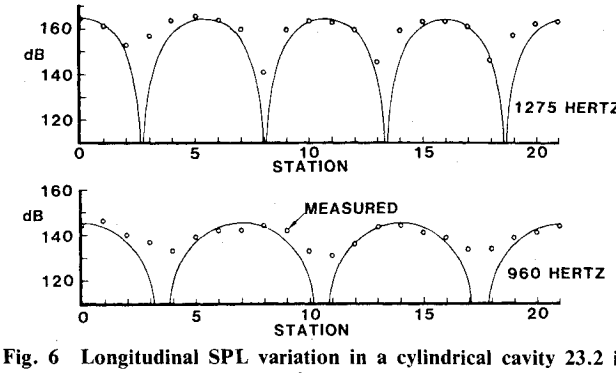

Fig. 6 Longitudinal SPL variation in a cylindrical cavity 23.2 in. long and 5.4 in. in diameter at 0.81 Mach number, 960 and 1275 Hz.

located at the downstream end of the cavity. The shear layer oscillation frequency given by the Rossiter equation is shown by the solid lines for $N_R = 1$, 2, and 3. The fore-aft acoustic resonance frequencies are shown by the lines for $N_x = 1$, 2, 3, 4, and 5. The frequencies at which strong cavity oscillation occurred are indicated by the solid symbols. Frequencies at which weaker oscillation occurred (weaker but still clearly an oscillatory condition) are indicated by the open symbols. From several such experiments, it was concluded that the shear layer instability or oscillation frequency increases with Mach number approximately in accord with the modified Rossiter equation. However, in the absence of any reinforcement from acoustic resonance, the shear layer oscillation is comparatively weak. At certain velocities when the shear layer oscillation frequency approaches an acoustic resonance frequency in the cavity, the shear layer oscillation sometimes "locks on" that acoustic resonance. Throughout a definite velocity range, the coupled shear layer/cavity oscillation occurs at the acoustic resonance frequency. During this "lock on" condition, the shear layer oscillation is reinforced and fluctuating pressures in the cavity become very intense.

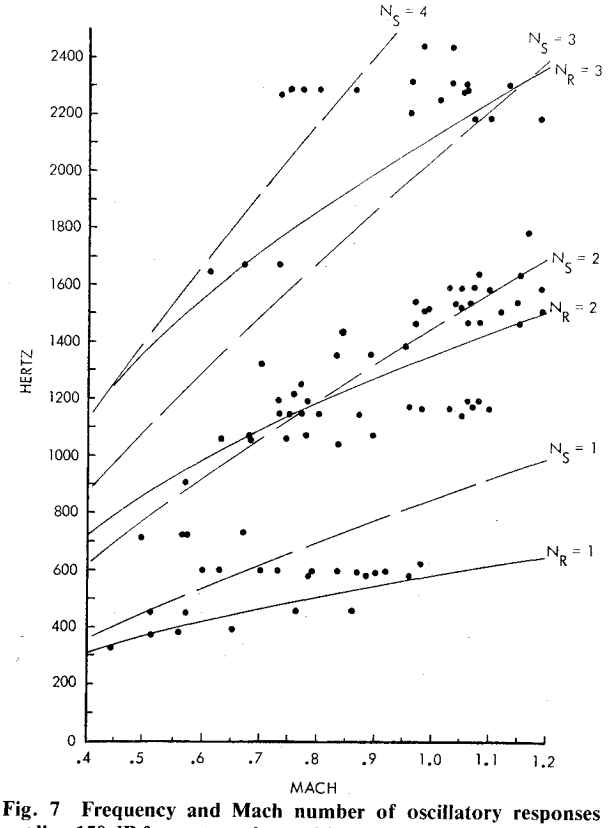

Fig. 7 Frequency and Mach number of oscillatory responses exceeding 150 dB for rectangular cavities.

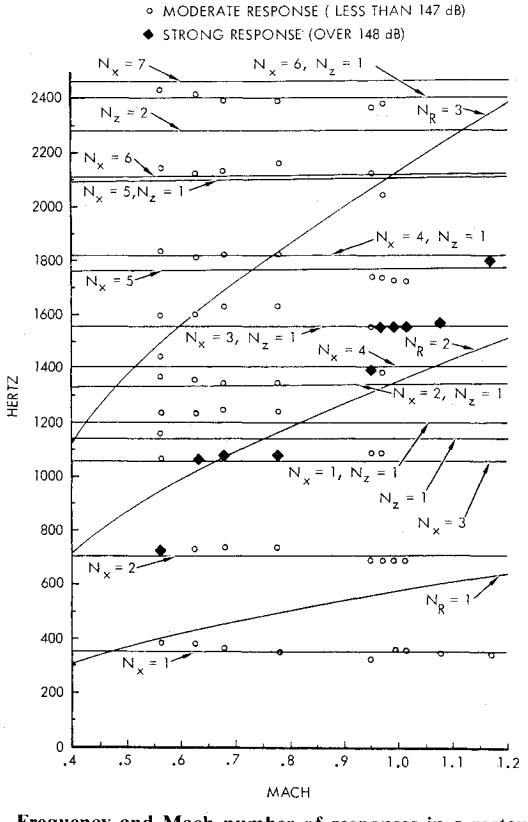

Fig. 8 Frequency and Mach number of responses in a rectangular cavity 18 in. long, 5.75 × 5.75 in.^{2}, with a 1 × 6-in. opening.

Prior investigators have offered different descriptions of the mechanism involved during this oscillatory condition. Some descriptions have dealt with flow turbulence, some with captive vortices in the cavity, some with pure vortex shedding, some with fluid inflow/outflow, and some with reversed flow

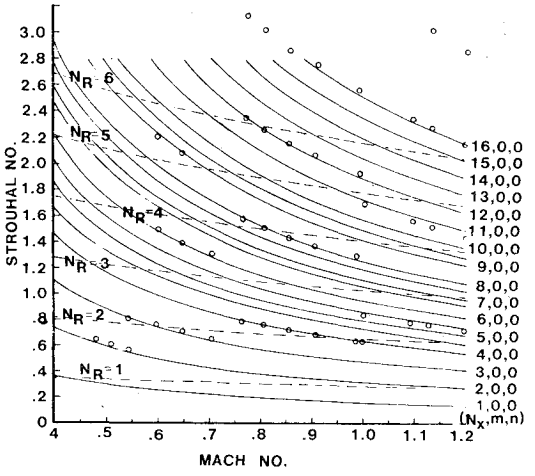

Fig. 9 Cavity oscillations for a cylindrical cavity.

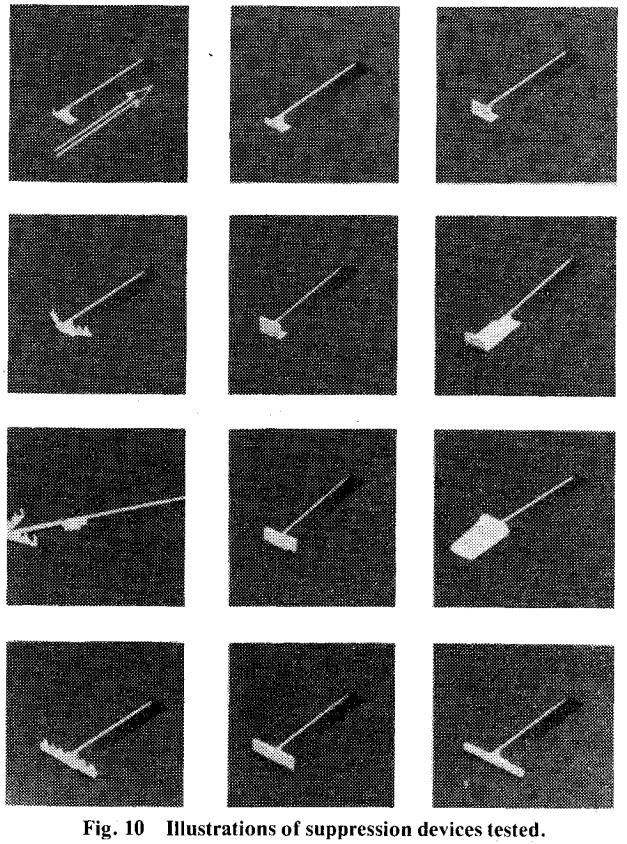

Fig. 10 Illustrations of suppression devices tested.

and forward propagating pressure disturbances within the cavity. From the current tests, it is believed that any of the previously described mechanisms can occur under the right circumstances. It is also believed that in some cases more complex mechanisms are involved. It was observed that strong oscillation occurred in cavity configurations where none of the aforementioned mechanisms seem plausible. As a result of many experiments, it was concluded that the formulation of prediction methods would first require a satisfactory means for quantifying the cavity acoustic resonance frequencies.

Acoustic resonances in a cavity are normal modes of vibration of the air filling the cavity volume, and hereinafter are sometimes called acoustic modes, or simply "modes." In any normal mode vibration system, an infinite number of resonant modes are possible. Any particular mode characterizes a particular spatial variation of the pressure in the air; likewise, a standing wave characterizes a particular acoustic

resonance. For large rectangular enclosures where the aperture open area is small relative to the surrounding wall area, the cavity can be treated as fully enclosed. The frequency is determined from

$$f=\frac{C}{2}\left[\left(\frac{N_x}{l_x}\right)^2+\left(\frac{N_z}{l_z}\right)^2\right]^{1/2} \tag{3}$$

where N_x and N_z are mode integers 1-4, etc., in the fore-aft direction and the depthwise direction, respectively; C is speed of sound in the cavity; and l_x and l_z are the cavity dimensions.

For cylindrical or semicylindrical enclosures with the diameter large in comparison to the aperture width, acoustic resonance frequency is given by

$$f=\frac{C}{2}\left[\left(\frac{N_x}{l_x}\right)^2+\left(\frac{\alpha_{mn}}{r}\right)^2\right]^{1/2} \tag{4}$$

where N_x is mode integer 1-4, etc., in the fore-aft direction; α_{mn} is a mode-dependent coefficient for the tangential and radial mode integers, m denotes tangential modes and n denotes radial modes; C is the speed of sound in the cavity; and r is the cylinder radius. In the interest of simplifying the use of these equations in predictions, it is advantageous to standardize Eqs. (3) and (4) to a single expression of the form

$$f=\frac{C}{2}\left(\frac{N_x^2}{l_x^2}+\frac{F^2}{l_F^2}\right)^{1/2} \tag{5}$$

where lateral acoustic modes have been neglected. For rectangular enclosures, $F=N_z=0$, 1, 2, 3, etc.; for cylindrical and semicylindrical enclosures, $F=\infty_{mn}$. Converting C, the speed of sound in the enclosures, to freestream speed of sound C_∞ gives

$$f=\frac{C_\infty}{2}(1+0.2M^2)^{1/2}\left(\frac{N_x^2}{l_x^2}+\frac{F^2}{l_F^2}\right)^{1/2} \tag{6}$$

The expression for the shear layer pressure oscillations, Eq. (1), in terms of Mach number becomes

$$f=\frac{MC_\infty}{L}\left[\frac{N_R-0.25}{M(1+0.2M^2)^{-1/2}+1.75}\right] \tag{7}$$

With Eqs. (6) and (7), the frequencies of the shear layer pressure oscillation and the various acoustic resonance modes in an enclosure can be calculated and plotted as a function of Mach number on a single plot as was done in Fig. 8.

If the possible frequencies of oscillations are needed for various values of C_∞, the curve plotting process and the identification of curve intersections can become extremely burdensome. It is therefore advantageous to normalize the frequency expressions in terms of Strouhal number and to make certain definitions and substitutions which simplify the calculations. The modified Rossiter equation for shear layer oscillation in terms of Strouhal number is

$$S=\frac{N_R-0.25}{M(1+0.2M^2)^{-1/2}+1.75} \tag{8}$$

The cavity acoustic resonance (recognizing that $S=fL_x/U$, and $C_\infty=U/M$) in terms of Strouhal number is

$$S=\frac{L_x(1+0.2M^2)^{1/2}}{2M}\left(\frac{N_x^2}{l_x^2}+\frac{F^2}{l_F^2}\right)^{1/2} \tag{9}$$

By definition, let

$$(1+0.2M^2)^{1/2}=H \tag{10}$$

and

$$L_x/l_x=a \qquad L_x/l_F+b \tag{11}$$

then

$$\left(\frac{N_x^2}{l_x^2}+\frac{F^2}{l_F^2}\right)^{1/2}=\frac{(a^2N_x^2+b^2F^2)^{1/2}}{L_x} \tag{12}$$

now

$$(a^2N_x^2+b^2F^2)^{1/2}=G \tag{13}$$

Then by substitution the modified Rossiter equation for shear layer oscillation in terms of Strouhal number is

$$S=\frac{N_R-0.25}{M/H+1.75} \tag{14}$$

and the cavity acoustic resonance in terms of Strouhal number is

$$S=GH/2M \tag{15}$$

By using Eqs. (14) and (15), shear layer oscillation modes and acoustic resonance modes can be calculated. Both modes along with test data are shown in Fig. 9. The intersections of the two sets of curves give the potential resonances. It is seen that when sustained cavity oscillation occurs, the measured Strouhal number tracks the calculated acoustic mode Strouhal number, and as speed increases, the cavity oscillation shifts as the shear layer oscillation Strouhal curve comes into the proximity of different acoustic modes.

At the intersections of the Strouhal curves for shear layer oscillation and acoustic resonance, i.e., where the two frequencies coincide,

$$\frac{N_R-0.25}{(M/H)_i+1.75}=\frac{GH_i}{2M_i} \tag{16}$$

where subscript i denotes intersection. By algebraic manipulation,

$$\left(\frac{H}{M}\right)_i=\frac{2(N_R-0.25)-G}{1.75G} \tag{17}$$

This is a useful interim form, in that the quantity $(H/M)_i$ involves only the intersection Mach number, and the right side involves only the dimensional and modal-order parameters relating to shear layer and acoustic resonance frequencies. Since, by definition,

$$\frac{H}{M}=\frac{(1+0.2M^2)^{1/2}}{M} \qquad \left(\frac{H}{M}\right)^2=\frac{1+0.2M^2}{M^2} \tag{18}$$

and by further manipulation, the intersection Mach number is

$$M_i=\left[\left(\frac{H}{M}\right)_i^2-0.2\right]^{-1/2} \tag{19}$$

From Eq. (15), the Strouhal number where intersection occurs is

$$S_i=\frac{G}{2}\left(\frac{H}{M}\right)_i \tag{20}$$

Suppression Devices

When the flow-induced acoustic levels in an enclosure become high enough to cause damage to the structure or internally stored components it is desirable to suppress the levels by some means. Based on flow observations using oil streaks, shadowgraphs, and water tables, some investigators have surmised that the introduction of turbulence into the shear layer could effectively destroy the shear layer and, therefore, suppress cavity oscillations. The thickness of the shear layer is increased by turbulence, and in some cases cavity oscillation sound pressure levels are reduced. The

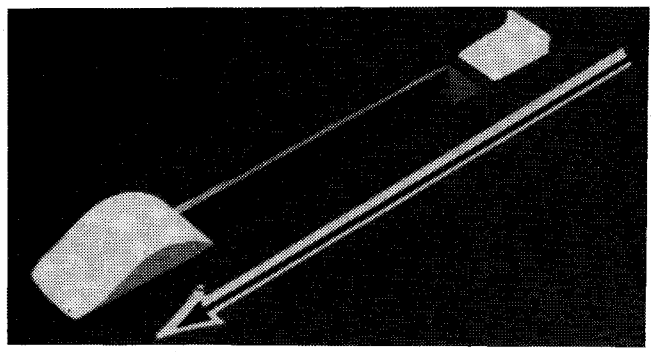

Fig. 11 Illustrations of selected suppression devices.

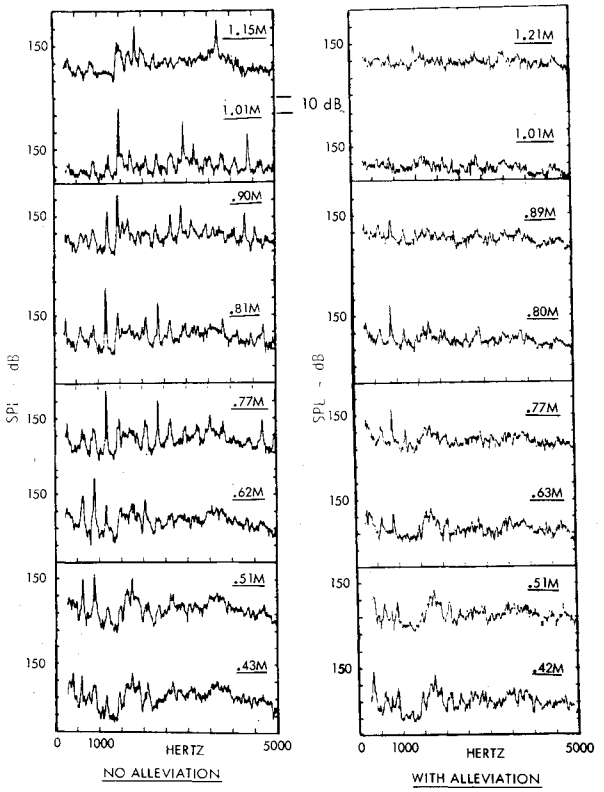

Fig. 12 Cylindrical cavity with and without spoiler/ramp suppression devices.

authors believe the basic reason for the effectiveness of some spoilers is that the inherent instability of the free shear layer is suppressed. The instability consists of an inflection point in the velocity profile. The addition of turbulence to the shear layer delays or reduces the amplitude of the inflection, thus resulting in a reduction of the shear layer oscillation amplitude. Solid and porous spoilers, leading- and trailing-edge airfoils and ramps, and combinations thereof have been used for suppression devices on cavities with large openings with various degrees of success. It was not known if the same type of spoilers would be effective for cavities with small openings, thus numerous devices were evaluated. Figure 10 shows 12 different configurations tested. The test results led to the observation that location, size, and orientation were more important than the degree of turbulence created by a particular device. In other words, a solid spoiler fence oriented normal to the flow at an optimized position upstream of the aperture leading edge might be more effective than a sawtooth device of similar overall geometric proportions.

Additional tests were conducted to evaluate an upstream spoiler with and without a downstream ramp. This configuration is shown in Fig. 11. Typical suppressed and unsuppressed data are presented in Fig. 12. From these tests it

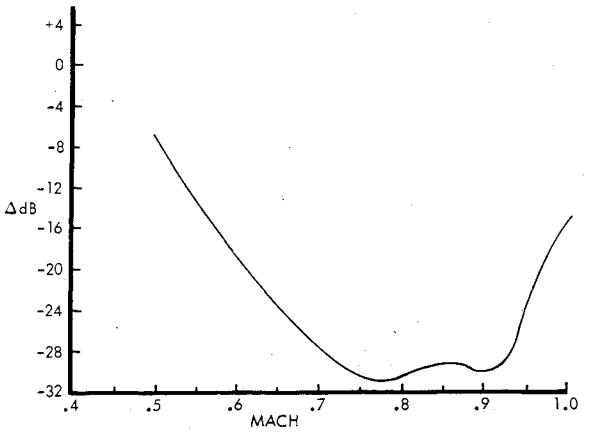

Fig. 13 Optimized suppression of maximum oscillatory SPL.

was observed that the upstream spoiler fence, when moved ahead of the aperture leading edge, evidently became the upstream origin for the shear layer. The shear layer characteristic length was thus increased, leading to a reduction in the shear layer oscillation frequency. Suppression was derived by "mismatching" or decoupling the shear layer from the responding acoustic mode. Ramps positioned downstream of the aperture present a condition whereby the characteristic length is indistinct. The unattached shear layer length changes as its point of reattachment wanders fore-aft on the sloped ramp surface. The "Rossiter" modal frequencies for the original aperture are thus altered. When no acoustic modes were available below the principle mode frequency, the suppression devices that increased "apparent" aperture length were very effective. In large enclosures with many acoustic modes below the principle cavity oscillation mode, an upstream spoiler and a downstream ramp usually caused the shear layer oscillation to couple with a lower-order acoustic mode. The effectiveness of this optimization process is displayed in Fig. 13, where it is seen that in the Mach number range of from 0.75 to 0.9 the maximum modal oscillatory level was suppressed 30 dB.

The test data collectively indicate that the spoiler height should be at least 7% of the aperture length, and position should be about 25% of the aperture length ahead of the aperture leading edge. The fore-aft position of the spoiler appears to be even more important than height. If an airfoil ramp is located downstream, the height of the ramp should be approximately equal to the height of the spoiler.

Summary and Conclusions

An investigation of the flow-induced pressure oscillations in large enclosures with small openings has been performed. Expressions have been developed which predict the frequencies of the pressure oscillation that occur in the enclosure. Also, expressions to predict the onset and termination Mach number for these oscillations have been developed. All of the enclosures tested with a small opening exposed to parallel freestream flow exhibited intense pressure oscillations.

One of the major findings was that the enclosure acoustic mode pressures appear to regulate the shear layer pressure oscillations, such that the shear layer can excite an acoustic mode over an appreciable Mach number range. However, the strongest oscillation occurs when the shear layer frequency coincides with an enclosure acoustic mode. The strongest acoustic mode usually involved the second shear layer mode.

The results demonstrated that the suppression devices applied to enclosures with large openings are also effective for enclosures with small openings. It has been shown for the first time that the effectiveness of the suppression devices can be optimized by selecting the proper fore-aft position relative to

the upstream and downstream edges of the opening. This position decouples the shear layer oscillation frequency from the enclosure modal frequencies. Further studies are needed to advance the understanding of the mechanisms involved in the way the acoustic pressure waves regulate the shear layer oscillation frequencies.

References

[1]Plumblee, H.E., Gibson, J.S., and Lassiter, L.W., "A Theoretical and Experimental Investigation of the Acoustical Response of Cavities in an Aerodynamic Flow," WADD-TR-61-75, U.S. Air Force, March 1962.

[2]Rossiter, J.E., "Wind Tunnel Experiments on the Flow Over Rectangular Cavities at Subsonic and Transonic Speeds," ARC R&M 3438, Oct. 1964.

[3]Heller, H.H., Holmes, G., and Covert, E.E., "Flow-Induced Pressure Oscillations in Shallow Cavities," AFFDL-TR-70-104, Dec. 1970.

[4]Smith, D.L. and Shaw, L.L, "Prediction of the Pressure Oscillations in Cavities Exposed to Aerodynamic Flow," AFFDL-TR-75-34, Oct. 1975.

[5]Bliss, D.B. and Hayden, R.E., "Landing Gear and Cavity Noise Prediction," NASA Contractor Report NASA CR-2714, 1976.

[6]Shaw, L.L. and Smith, D.L., "Aero-Acoustic Environment of a Store in an Aircraft Weapons Bay," AFFDL-TR-77-18, March 1977.

[7]Block, P.J.W., "Measurements of the Tonal Component of Cavity Noise and Comparison with Theory," NASA TP-1013, 1977.

[8]Tam, C.K.W. and Block, P.W., "On Tones and Pressure Oscillations Induced by Flows Over Rectangular Cavities," *Journal of Fluid Mechanics,* Vol. 89, Nov. 1978.

[9]Rockwell, D. and Naudascher, E., "Review-Self-Sustaining Oscillations of Flow Past Cavities," *Transactions of the ASME,* Vol. 100, June 1978, pp. 152-165.

[10]Heller, H.H. and Bliss, D.B., "Aerodynamically Induced Pressure Oscillations in Cavities—Physical Mechanisms and Suppression Concepts," AFFDL-TR-74-133, Feb. 1975.

[11]Shaw, L.L., "Suppression of Aerodynamically Induced Cavity Pressure Oscillations," AFFDL-TR-79-3119, Nov. 1979.

[12]Nyborg, W.L., "Self-Maintained Oscillations in a Jet Edge System," *Journal of the Acoustical Society of America,* Vol. 26, March 1954, pp. 174-182.

[13]Spee, B.M., "Wind Tunnel Experiments on Unsteady Cavity Flow at High Subsonic Speeds, Separated Flows," Part II, AGARD CP No. 4, May 1966, pp. 941-974.